Spectrum Blind Unlimited Sampling of Multi-Band Signals

Ruiming Guo and Ayush Bhandari

Dept. of Electrical and Electronic Engg., Imperial College London, SW7 2AZ, UK.

{ruiming.guo,a.bhandari}@imperial.ac.uk

Abstract—**Recovering multiband spectra from sub-Nyquist sampling is a prominent research area in signal processing, driven by its wide range of applications and the technical challenges it presents. These challenges demand novel algorithmic approaches tailored to specific scenarios. The problem becomes even more complex when spectral locations are unknown, leading to the development of Blind Multi-Band Sampling techniques. Despite several proposed solutions, a notable research gap persists. Signals with varying energies across different spectral bands often exhibit high-dynamic-range (HDR) features, and with a fixed bit budget, there is a trade-off between optimizing digital resolution and spanning HDR. In this paper, we address this challenge by leveraging the Unlimited Sensing Framework (USF). The interaction between modulo non-linearity and sub-Nyquist sampling induces aliasing in both the domain and range of the signal, further complicating the recovery process, especially with unknown spectral locations. To tackle these challenges, we propose a novel algorithm for blind multiband spectrum recovery from folded samples at sub-Nyquist rates. Importantly, we provide a theoretically guaranteed, perfect recovery at sub-Nyquist sampling rates. Our proof is constructive and leads to an efficient algorithm supported by a novel multi-channel sampling architecture. We validate our approach through numerical experiments, opening up new directions in theory, algorithms, and real-world applications for the field.**

Index Terms—**Blind spectrum sensing, multiband, nonuniform periodic sampling, sub-Nyquist sampling, unlimited sampling.**

I. Introduction

Digitization and Nyquist Rate. The well-known Shannon-Nyquist framework lays the foundation for the conventional digital acquisition protocol, which catalyzed the so-called "digital revolution". The Shannon sampling theorem links continuous-time, bandlimited signal with discrete representation utilizing its amplitude samples taken at or above the Nyquist rate. This allows a perfect reconstruction and signal processing in a digital framework. This constitutes the current Shannon sampling paradigm for which its practical implementation leverages analog-to-digital convertors (ADCs).

Spectrum-Blind Multiband Recovery at Sub-Nyquist Rate. In this paper, we consider the class of multiband signals, whose spectral support resides within several continuous passbands, spread over a wide spectrum. This model naturally arises when capturing a sum of narrowband signals which are modulated by carriers with different, high frequencies. Fig. 1 schematically depicts a typical spectral support of a multiband signal, which is mathematically defined by

$$f(t) = \varphi(t) \sum_{k=0}^{K-1} c_k e^{j\omega_k t}, \quad \varphi \in \mathcal{B}_\Omega, \quad f \in \mathbb{R} \qquad (1)$$

$\varphi(t)$ is bandlimited with bandwidth 2Ω. $\{\omega_k\}_{k=0}^{K-1}$ are *unknown* carrier frequencies satisfying $\min_k |\omega_k| > 2\Omega$. Such kind of signals are at the core of various applications, with examples ranging from cognitive radio [1], RF communication [2], optical fiber communications [3] to orthogonal frequency-division multiplexing communications [4]. It is well-documented that the sampling rate and the
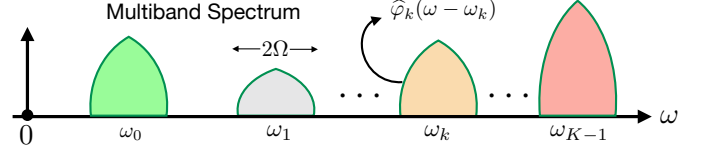
Fig. 1: Typical spectrum support of a multiband signal $f(t)$.

bit-budget for quantization dictate the sampling cost of the ADCs. As multiband signals are intrinsically featured with high bandwidth, the conventional Nyquist sampling thus becomes infeasible due to high power consumption. This motivates the development of the so-called sub-Nyquist sampling [2], [5]–[12].

Related Work. Current methods on sub-Nyquist multiband spectrum sensing can be divided into the following two categories:

1) Known-Spectrum Techniques. Uniform sampling a real bandpass signal at low-rate was considered in [13]. Lin and Vaidyanathan utilized periodic non-uniform sampling approach to multiband signals in [14]. These methods enable perfect recovery at rates approaching that derived by Landau [15].
2) Blind-Spectrum Techniques. Reconstruction under partial knowledge of the spectral support was studied in [8], [9], [16]. These works use a multi-coset architecture and assume a certain mathematical condition on band locations instead of requiring the exact support. Herley and Wong [17] suggested a half-blind sampling system. Similar ideas were later suggested in [7]. A spectrum-blind method that ensures perfect reconstruction was reported by Mishali and Eldar in [2]. This approach utilizes compressed sensing tools and allow recovery with arbitrary band locations.

In essence, sub-Nyquist multiband recovery focuses on "unfolding" of spectrum that is "aliased" in the Fourier domain.

Concurrent Unfolding along Amplitude and Spectrum. In another incarnation, this unfolding problem is also at the heart of the Unlimited Sensing Framework (USF) [18]–[21]. Different from sub-Nyquist sampling, in the USF, folding is *purposefully* introduced to achieve folding of amplitude, thus eliminating ADC clipping or saturation. Increasing the dynamic range of ADCs may also avoid this issue, but would inevitably result in poor digital resolution due to quantization. In a nutshell, the conventional Shannon-Nyquist framework encounters a fundamental trade-off between dynamic range and digital resolution, which is overcome by the USF. In the USF, on the hardware front, a modulo non-linearity of the form

$$\mathscr{M}_\lambda : g \mapsto 2\lambda \left(\left[\!\left[\frac{g}{2\lambda} + \frac{1}{2} \right]\!\right] - \frac{1}{2} \right), \quad [\![g]\!] \overset{\text{def}}{=} g - \lfloor g \rfloor \qquad (2)$$

where $\lfloor g \rfloor = \sup\{k \in \mathbb{Z} \,|\, k \leqslant g\}$ (floor function) is injected in the analog domain, before performing pointwise sampling. The first hardware prototype was shown in [21]. On the algorithm front, novel, mathematically guaranteed, recovery algorithms are used to attain the "inversion" of the $\mathscr{M}_\lambda(\cdot)$ operation, enabling recovery of HDR signal from its low-dynamic-range (LDR), modulo samples [21], [22].

USF fundamentally simultaneously achieve HDR and high digital resolution, providing a performance breakthrough in 1) up to 25λ to 30λ [20] dynamic range improvement in the presence of non-idealities, system noise and quantization; 2) 10-12 dB improvement in the quantization noise floor over the conventional ADC, in the context of radars [23] and tomography [24], and 3) higher-order modulation schemes in MIMO communications in [25], *e.g.* 1024 QAM. USF essentially shares the same "unfolding" flavor as sub-Nyquist multiband reconstruction, but the subtlety here is the distinction that arises between spectrum and amplitude [10]–[12]. While sub-Nyquist acquisition is our ultimate goal, we know that reconstruction methods at the core of USF require oversampling [19], [20], [22]. Hence, sub-Nyquist acquisition results in a fundamental contradiction instigating a stalemate between *analysis* and *synthesis*, creating challenges for multiband recovery from sub-Nyquist, folded samples.

Contributions. We have previously studied the sub-Nyquist USF for bandpass signals [26] and sums of sinusoids [10]–[12], which are special cases of multiband signal class. In this paper, we consider the *blind* multiband reconstruction with sub-Nyquist, modulo samples. The solution to this problem would directly translate to several benefits since we can 1) reduce sampling cost due to sub-Nyquist rate and low voltage ranges of modulo ADCs [25], 2) prevent saturation or clipping arising from HDR input signals [21], and 3) achieve high digital resolution with a given quantization bit-budget [23].

The key contributions of this work are as follows:

C_1) We propose a novel sampling scheme that allow blind multiband recovery from sub-Nyquist, modulo samples. This is very different from previous works which primarily focused on subsets of multiband signal class [12], [26].

C_2) Our recovery method is theoretically guaranteed and leads to perfect signal reconstruction, independent of band locations. We validate our method through extensive numerical experiments, demonstrating its effectiveness and accuracy.

Notation. Integers, reals, and complex numbers are denoted by $\mathbb{Z}, \mathbb{R}$ and $\mathbb{C}$, respectively. We use $\mathbb{I}_N = \{0, \cdots, N-1\}, N \in \mathbb{Z}^+$ to denote the set of N contiguous integers. Vectors and matrices are written in bold lowercase and uppercase fonts., *e.g.* $\mathbf{f} \in \mathbb{R}^N$ and $\mathbf{F} \in \mathbb{R}^{N \times M}$. The max-norm of a function is defined as, $\|f\|_\infty = \inf\{c_0 \geqslant 0 : |f(t)| \leqslant c_0\}$; for sequences, $\|f\|_\infty = \max_n |f[n]|$. Function derivative is denoted by $f'(t)$.

II. Blind Sub-Nyquist Multiband USF

Problem Formulation. We consider the multiband signal model in (1), where the spectral support and φ are both *unknown*[1]. As a paradigm shift from the traditional sampling architecture, in USF, the action of modulo non-linearity converts $f(t)$ to a folded, continuous-time signal, $y(t) = \mathscr{M}_\lambda(f(t))$. Then, $y(t)$ is sampled in a pointwise fashion, leading to modulo samples $y[n] = \mathscr{M}_\lambda(f(t))|_{t=nT}, n \in \mathbb{I}_N$ where $T = 1/f_s$ is the sampling step. Given $\{y[n]\}_{n=0}^{N-1}$, our goal is to retrieve $f(t)$ at sub-Nyquist rate.

Mathematical Model of the Sampling Pipeline. We extend the multi-coset (MC) sampling architecture to USF context to tackle these technical challenges. Denote by f_n^l the MC signal samples

$$f_n^l = \text{III}_f(nT + lT_d) \tag{3}$$

$$\text{III}_f(t) = \int_{t-\epsilon}^{t+\epsilon} \sum_{n \in \mathbb{Z}} \sum_{l \in \mathbb{I}_{L+1}} f(\tau) \delta(\tau - nT - lT_d) d\tau, \quad \epsilon > 0$$

[1] *i.e.* the carrier frequencies $\{\omega_k\}_{k=0}^{K-1}$ are *unknown* prior to sampling.

where T_d is the time-delay and $\text{III}_f(t)$ is multi-coset operator. n and l denote the sample and channel indices, respectively. Similarly, denote by y_n^l the MC modulo samples, $y_n^l = \text{III}_y(nT + lT_d)$. Let $\varphi_n^l = \text{III}_\varphi(nT + lT_d)$, $\varphi_n = \varphi(t + (L-1)T_d/2)|_{t=nT}$ and $\Omega_K = \|\omega_k\|_\infty$. Denote by $\underline{f}_n^l$ the finite-difference of f_n^l, *i.e.* $\underline{f}_n^l \overset{\text{def}}{=} f_n^{l+1} - f_n^l$.

Overview of the Recovery Strategy Since each channel is under-sampled, existing USF approaches that typically rely on chanel-wise oversampling cannot be applied [19]–[21]. Nonetheless, the folding non-linearity $\mathscr{M}_\lambda(\cdot)$ is possible to be decoupled and inverted along *channel* dimension. The key insight being that f_n^l is a temporal-spatial signal, its spatial variation across channels is upper bounded, provided that T_d is sufficiently small. This spatial structure enables the inversion of $\mathscr{M}_\lambda(\cdot)$ via non-linear filtering of amplitudes similar to the operation in [19] (see Theorem 1), resulting in the recovery of $\underline{f}_n^l$. With $\underline{f}_n^l$ known, we demonstrate that $\underline{f}_n^l$ can be approximated by a finite sum of complex exponentials up to a bounded error. As a result, the carrier frequencies $\{\omega_k\}_{k=0}^{K-1}$ can be estimated up to a bounded standard deviation.

Due to the modulo non-linearity $\mathscr{M}_\lambda(\cdot)$, f_n^l can only be recovered up to an *unknown* constant by performing anti-difference operator on $\underline{f}_n^l$. This motivates the design of a direct recovery approach in finite-difference domain. With spectrum support known from $\{\omega_k\}_{k=0}^{K-1}$ and Ω, our key finding is that, one can perfectly reconstruct $f(t)$ from $\{\underline{f}_n^l\}_{n \in \mathbb{I}_N}^{l \in \mathbb{I}_L}$, under appropriate hypotheses.

Blind Carrier Frequency Estimation. The result is as follows:

Theorem 1. *Let $f(t)$ be a multiband signal defined in (1). Given MC modulo samples $\{y_n^l\}_{n \in \mathbb{I}_N}^{l \in \mathbb{I}_{L+1}}$ defined above. Then, $\{c_k, \omega_k\}_{k=0}^{K-1}$ can be retrieved with an error of standard deviation*

$$\begin{aligned}
\text{std}\{\omega_k\} &\leqslant \frac{\sqrt{6}\gamma\Omega\|f\|_\infty}{2L^{3/2}|c_k|\|\varphi_n\|_\infty \sin\frac{|\omega_k|T_d}{2}} \\
\text{std}\{|c_k|\} &\leqslant \frac{\gamma\Omega T_d \|f\|_\infty}{2\sqrt{2L}\|\varphi_n\|_\infty \sin\frac{|\omega_k|T_d}{2}}
\end{aligned} \tag{4}$$

if $L \geqslant 2K$, $T_d \leqslant \pi/\Omega_K$ and $\beta \leqslant \lambda/\|f\|_\infty$, where β and γ are defined by $\beta \overset{\text{def}}{=} 2\sin\left(\frac{\Omega_K T_d}{2}\right) + \Omega T_d$ and $\gamma \overset{\text{def}}{=} 1 + (L-1)\sin\frac{\Omega_K T_d}{2}$.

Proof. We present the proof of this theorem by constructing the solution to the carrier frequency estimation problem.

i) Inversion of Range Folding. Denote by $\underline{f}_n^l$ the finite-difference of f_n^l along channel dimension, we have ($n \in \mathbb{I}_N, l \in \mathbb{I}_L$)

$$\underline{f}_n^l \overset{\text{def}}{=} f_n^{l+1} - f_n^l = \sum_{k=0}^{K-1} c_k e^{j\omega_k(nT + lT_d)} h_n^l \tag{5}$$

where $h_n^l = \varphi_n^{l+1} e^{j\omega_k T_d} - \varphi_n^l$ and is bounded, $|h_n^l| \leqslant |\varphi_n^{l+1} - \varphi_n^l| + |\varphi_n^{l+1}| |e^{j\omega_k T_d} - 1|$. From the Bernstein's inequality, we know that $|\varphi_n^{l+1} - \varphi_n^l| = \left|\int_{lT_d}^{(l+1)T_d} \varphi'(t + nT)dt\right| \leqslant \Omega \|\varphi\|_\infty T_d$. It suffices to show that $|e^{j\omega_k T_d} - 1| = 2\left|\sin\frac{\omega_k T_d}{2}\right|$. Hence, h_n^l is bounded by $|h_n^l| \leqslant \left(2\sin\frac{\Omega_K T_d}{2} + \Omega T_d\right)\|\varphi\|_\infty$. Let $\beta = 2\sin\frac{\Omega_K T_d}{2} + \Omega T_d$. Thus, $\underline{f}_n^l$ in (5) is bounded by $|\underline{f}_n^l| \leqslant \sum_{k=0}^{K-1} |c_k| |h_n^l| \leqslant \|c_k\|_{\ell_1} \beta \|\varphi\|_\infty$. Notice that, $\|f\|_\infty = \|\varphi\|_\infty \|c_k\|_{\ell_1}$, which eventually results in $|\underline{f}_n^l| \leqslant \beta \|f\|_\infty$. From the modular decomposition property [19], [20], [22], we have $f = \mathscr{M}_\lambda(f) + \varepsilon_f, \varepsilon_f(t) = \sum_{m \in M_\lambda} c_m \mathbb{1}_{\mathcal{D}_m}(t)$ where $c_m \in 2\lambda\mathbb{Z}$. ε_f is the residue function and $\mathbb{1}_{\mathcal{D}}$ is the indicator function on domain D. Then, we have $\mathscr{M}_\lambda(y_n^{l+1} - y_n^l) = \mathscr{M}_\lambda(\mathscr{M}_\lambda(f_n^{l+1} - f_n^l) + \mathscr{M}_\lambda(\varepsilon_{f_n^l} - \varepsilon_{f_n^{l+1}})) = \mathscr{M}_\lambda(f_n^{l+1} - f_n^l) = \mathscr{M}_\lambda(\underline{f}_n^l)$. If T_d is small enough, then we have

$$\beta \leqslant \lambda/\|f\|_\infty \mapsto \mathscr{M}_\lambda(y_n^{l+1} - y_n^l) = \underline{f}_n^l \tag{6}$$
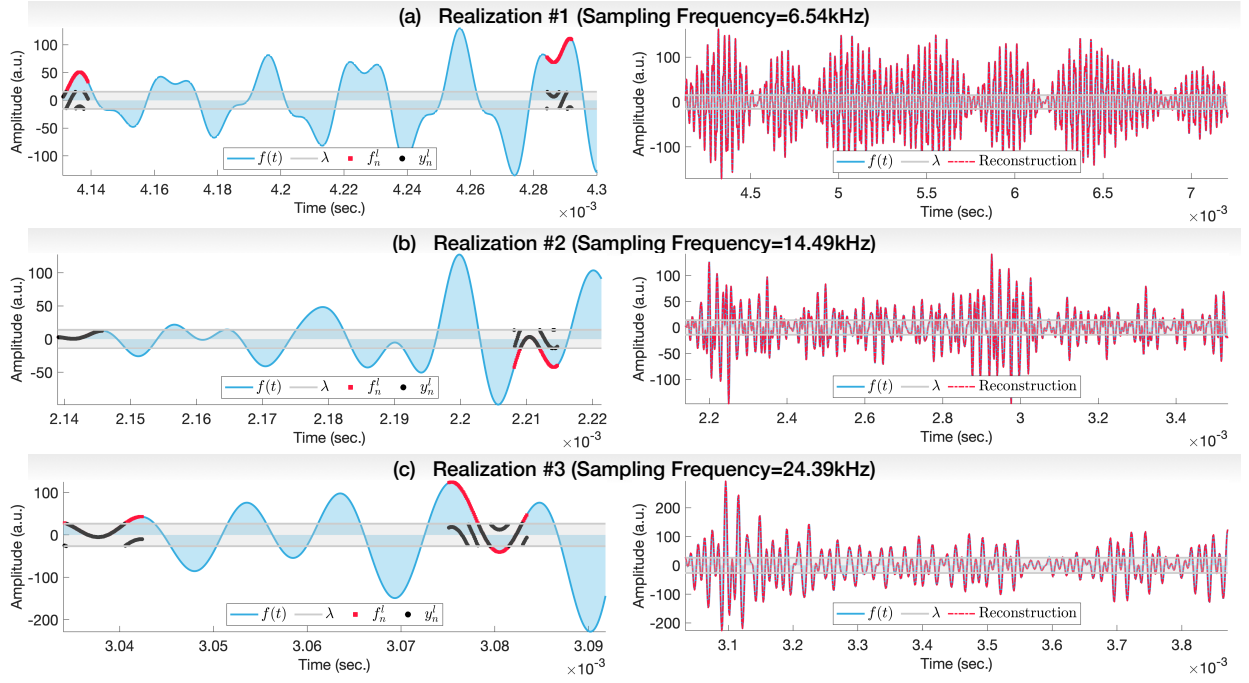
Fig. 2: Numerical validations. The carrier frequencies lie in hundred kilohertz range with kilohertz scale sampling rate. We conduct 3 experiments with different maximal frequency $B = \frac{\Omega}{2\pi}$ of φ: (a) 4.18 kHz, (b) 12.36 kHz, and (c) 19.54 kHz. In all realizations, the reconstruction is accurate with $\mathcal{E}_2\big(\mathbf{f}, \widetilde{\mathbf{f}}\big) < 2 \times 10^{-7}$.

which enables range unfolding independent of the sampling rate T.

ii) Signal Approximation with Bounded Error. Notice that, $\{\underline{f}_n^l\}_{l \in \mathbb{I}_L}$ in (5) can be approximated by $\widetilde{g}_n^l = \sum_{k=0}^{K-1} a_{k,n} e^{\jmath \omega_k T_d l}$ where $a_{k,n} = c_k \varphi_n e^{\jmath \omega_k T n} \big(e^{\jmath \omega_k T_d} - 1\big)$. And the approximation error between $\underline{f}_n^l$ and $\widetilde{g}_n^l$ is upper bounded by $\left|\underline{f}_n^l - \widetilde{g}_n^l\right| \leqslant \left|\underline{f}_n^l - \underline{g}_n^l\right| + \left|\underline{g}_n^l - \widetilde{g}_n^l\right|$ where the auxiliary variable $\underline{g}_n^l$ is defined as $\underline{g}_n^l = \sum_{k=0}^{K-1} c_k \varphi_n^l e^{\jmath \omega_k T n} \big(e^{\jmath \omega_k T_d} - 1\big) e^{\jmath \omega_k T_d l}$. With $\underline{g}_n^l$, we further have that $\left|\underline{f}_n^l - \underline{g}_n^l\right| \leqslant \left|\varphi_n^{l+1} - \varphi_n^l\right| \|c_k\|_{\ell_1} \leqslant \Omega T_d \|f\|_{\infty}$ and $\left|\underline{g}_n^l - \widetilde{g}_n^l\right| \leqslant \left|\varphi_n - \varphi_n^l\right| \|c_k\|_{\ell_1} 2\sin\frac{\Omega_K T_d}{2}$, which results in the bounded approximation error characterized by

$$\sigma_g \overset{\text{def}}{=} \left\|\underline{f}_n^l - \widetilde{g}_n^l\right\|_{\infty} \leqslant \left(1 + (L-1)\sin\frac{\Omega_K T_d}{2}\right) \Omega T_d \|f\|_{\infty} \quad (7)$$

To eliminate the frequency aliasing, we require that, $T_d \leqslant \pi/\Omega_K$. In what follows, we reinterpret σ_g as the standard deviation of an additive Gaussian noise characterizing the *uncertainty* induced by the model approximation inaccuracy.

iii) Blind Spectrum Parameter Estimation. With the approximation, $\underline{f}_n^l$ in (5) can be re-expressed as

$$\underline{f}_n^l = \sum_{k=0}^{K-1} a_{k,n} e^{\jmath \omega_k T_d l} + \eta_n^l, \quad \left\|\eta_n^l\right\|_{\infty} \overset{(7)}{\leqslant} \sigma_g, \quad l \in \mathbb{I}_L \quad (8)$$

Given the samples $\{\underline{f}_n^l\}_{l \in \mathbb{I}_L}$, estimating $\{a_{k,n}, \omega_k\}_{k \in \mathbb{I}_K}$ is the classical spectral estimation problem. We consider the uncertainties on the estimated frequencies and amplitudes $\{a_{k,n}, \omega_k\}_{k \in \mathbb{I}_K}$, resulting from the uncertainty on the samples, namely η_n^l.

To this end, we compute the Cramér-Rao Lower Bound (CRLB) of a frequency estimation problem, under additive white Gaussian noise of variance σ_g. As shown in [27]–[29], it is sufficient to consider the Cramér-Rao bound for individual frequencies, provided that the frequencies are well-separated. Such kind of result naturally holds in the multiband context, since the carrier frequencies are generally

widely separated in the spectrum. Denote by $\text{std}\{\omega_k\}$ the standard deviation of the error of estimating a 1D frequency ω_k, associated with an amplitude $|a_{k,n}|$, the Cramér-Rao lower bound reads

$$\text{std}\{\omega_k\} \geqslant \frac{\sqrt{6}\sigma_g}{T_d |a_{k,n}| L^{3/2}}, \quad \text{std}\{|a_{k,n}|\} \geqslant \frac{\sigma_g}{\sqrt{2L}} \quad (9)$$

and the proof can be found in [30], [31]. It is well-known that the accuracy of algorithms like the maximum likelihood estimator (MLE) reach CRLB empirically for a large range of noise variances and asymptotically, when the number of samples L, tends to infinity [28], [32], [33]. This means, if such efficient algorithms are used and L is large enough, this inequality is, for all practical purposes, an equality

$$\text{std}\{\omega_k\} = \frac{\sqrt{6}\sigma_g}{T_d |a_{k,n}| L^{3/2}}, \quad \text{std}\{|a_{k,n}|\} = \frac{\sigma_g}{\sqrt{2L}} \quad (10)$$

for all frequency indices k. Combining (7), the estimation uncertainties on spectrum parameters $\{\omega_k, |a_{k,n}|\}_{k=0}^{K-1}$ are bounded by

$$\text{std}\{\omega_k\} \leqslant \frac{\sqrt{6}\gamma\Omega \|f\|_{\infty}}{|a_{k,n}| L^{3/2}}, \quad \text{std}\{|a_{k,n}|\} \leqslant \frac{\gamma\Omega T_d \|f\|_{\infty}}{\sqrt{2L}}. \quad (11)$$

Notice that, $a_{k,n} = c_k \varphi_n e^{\jmath \omega_k T n} \big(e^{\jmath \omega_k T_d} - 1\big)$. Hence, we have the result shown in (4), which completes the proof of Theorem 1. $\square$

Multiband Signal Recovery in Finite-Difference Domain. With $\underline{f}_n^l$ known, we reconstruct $f(t)$ via the following result:

Theorem 2. *Let $f(t)$ be a multiband signal defined in* (1). *Assume* $\min_k |\omega_k| > \Omega_s \overset{\text{def}}{=} 2\Omega + 2\Omega_e, \Omega_e \overset{\text{def}}{=} \max_k \frac{\sqrt{6}\gamma\Omega \|f\|_{\infty}|c_k|^{-1}}{2L^{\frac{3}{2}} \|\varphi_n\|_{\infty}\sin\frac{|\omega_k| T_d}{2}}$. *Let y_n^l denote the MC modulo samples defined above. Let $T = MT_d, M \in \mathbb{Z}^+$. Then, $f(t)$ can be exactly reconstructed if $T_d <$*

TABLE I: Summary of Experimental Parameters and Performance Evaluation.

Figure	B	f_s	L	λ	$\|f\|_\infty$	f_k	$\widetilde{f}_k$	$\mathcal{E}_2\big(\mathbf{f}, \widetilde{\mathbf{f}}\big)$
	(kHz)	(kHz)				(kHz)	(kHz)	
Fig. 2 (a)	4.18	6.54	47	15.42	171.03	$[31.39, 61.29, 81.54]$	$[31.72, 63.11, 81.97]$	4.65×10^{-11}
Fig. 2 (b)	12.36	14.49	59	14.03	146.67	$[48.97, 89.09, 109.69]$	$[49.89, 90.47, 112.74]$	8.20×10^{-12}
Fig. 2 (c)	19.54	24.39	83	26.54	292.63	$[56.21, 96.27, 109.68]$	$[55.24, 94.01, 113.55]$	2.88×10^{-17}

Algorithm 1 Blind sub-Nyquist USF Multiband Recovery

Input: Modulo Measurements y_n^l, K and Ω
1: Recover $\{\underline{f}_n^l\}_{n \in \mathbb{I}_N}^{l \in \mathbb{I}_L}$ via (6).
2: Given (8), estimate $\{\omega_k\}_{k=0}^{K-1}$ using spectral estimation.
3: Reconstruct $f(t)$ via Theorem 2.
Output: The recovered multiband signal $f(t)$.

$\frac{\min(\pi, \lambda/\|f\|_\infty)}{\Omega_K + \Omega}$, $N \to \infty$, $L \geqslant 2K$, $M < \frac{2\pi}{\Omega_s T_d}$ *and the matrix* $\mathbf{A} = [e^{j\frac{2ml\pi}{M}}]_{l \in \mathbb{I}_L}^{m \in \mathbb{I}_M}$ *has a fully Kruskal-rank*[2].

Proof. Given the modulo samples, from Theorem 1, we can exactly recover $\underline{f}_n^l$, and $\{\widetilde{\omega}_k\}_{k=0}^{K-1}$ up to an error bounded by $(\Omega_s - 2\Omega)/2$. The spectrum support estimate, $\mathcal{S}(f) = \bigcup_k S_i$, $S_i = \{\omega | |\omega - \widetilde{\omega}_k| \leqslant \Omega_s/2\}$, is known, which includes the spectral support of f. Denote by F the Fourier transform of f, then, we have $F(\omega) = 0, \forall \omega \notin \mathcal{S}(f)$. It suffices to show that, f is $(\Omega_K + \Omega)$-bandlimited. Since $g \in \mathbb{R}, T_d < \pi/(\Omega_K + \Omega)$, then $\mathcal{S}(f) \subsetneq [-\frac{\pi}{T_d}, \frac{\pi}{T_d}]$. From the Poisson summation formula, we have that $\sum_{n \in \mathbb{Z}} f_n^l e^{-jMn\omega T_d} = \sum_{m \in \mathbb{I}_M} \frac{e^{j\frac{2ml\pi}{M}}}{MT_d} F\left(\omega + \frac{2m\pi}{MT_d}\right)$. Hence, $\sum_{n \in \mathbb{Z}} \underline{f}_n^l e^{-jMn\omega T_d} = \sum_{m=0}^{M-1} \frac{e^{j\frac{2ml\pi}{M}}(e^{j\frac{2m\pi}{M}}-1)}{MT_d} F\left(\omega + \frac{2m\pi}{MT_d}\right)$, $\forall \omega \in [-\frac{\pi}{MT_d}, \frac{\pi}{MT_d}), l \in \mathbb{I}_L$. From the assumptions, $\min_k |\omega_k| > \Omega_s$ and $M < \frac{2\pi}{\Omega_s T_d}$, we show $\exists T_d < \frac{\pi}{\Omega_K + \Omega}$, s./t. $\min_k |\omega_k| - \frac{\Omega_s}{2} > \frac{\pi}{T_d M} > \frac{\Omega_s}{2}$, resulting in $F(\omega) = 0, \forall \omega \in [-\frac{\pi}{MT_d}, \frac{\pi}{MT_d})$. Hence,

$$\sum_{n \in \mathbb{Z}} \underline{f}_n^l e^{-jMn\omega T_d} = \sum_{m=1}^{M-1} \frac{e^{j\frac{2ml\pi}{M}}(e^{j\frac{2m\pi}{M}}-1)}{MT_d} F\left(\omega + \frac{2m\pi}{MT_d}\right).$$

Since $\mathbf{A}$ has a fully Kruskal-rank, the sampling pattern associated with III. $(nT + lT_d)$ is thus universal [7]. This results in a linear system of equations with *at most* K non-zero unknowns, since $M < \frac{2\pi}{\Omega_s T_d}$. $\mathcal{S}(f)$ indicates the support indices of $\mathbf{F}$, leading to a unique solution if $L \geqslant K$. With $F(\omega), \omega \in [-\frac{\pi}{T_d}, \frac{\pi}{T_d}]$, we can perfectly reconstruct $f(t)$ via the methods stated in [2], [9], [16]. □

An algorithmic implementation is provided in Algorithm 1.

III. Experiments

To validate Theorem 2, we conduct the following experiments:
- Dependence of the estimation error on number of channels L.
- Dependence of the reconstruction error on the bandwidth 2Ω.

For the ease of understanding, denote by $B = \frac{\Omega}{2\pi}$ and $f_k = \frac{\omega_k}{2\pi}$ the maximal frequency and carrier frequency in Hz, respectively. We use the mean squared error (MSE) $\mathcal{E}_2\big(\mathbf{f}, \widetilde{\mathbf{f}}\big) \overset{\text{def}}{=} \frac{1}{N} \sum_{n=0}^{N-1} \left|f[n] - \widetilde{f}[n]\right|^2$ to characterize reconstruction accuracy.

Effect of L. We perform three experiments to show how signal reconstruction error changes with number of channels. We fix the carrier amplitudes $\{c_k\}_{k=0}^{K-1}$ and increases the carrier frequency range. The experimental parameters and results are tabulated in Table

---

[2]The Kruskal-rank of a matrix $\mathbf{A}$ is defined as the maximal value L such that every set of L columns of $\mathbf{A}$ is linearly independent.
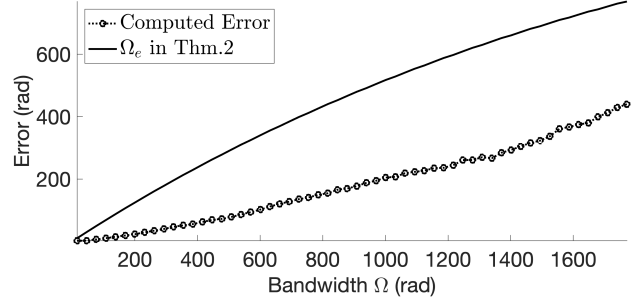

Fig. 3: Estimation error vs Ω. Each data point is the average of 1000 independent tests with random $\angle c_k$ (fixed $|c_k|$). The computed estimation error falls below the predictor Ω_e, validating the result in Theorem 1.

I. Fig. 2 depicts the modulo sampling and signal reconstruction under different sampling rates. From the experiments in Fig. 2 (b) and (c), It can be observed that the increase in L leads to a comparable frequency estimation accuracy. As shown in the last column of Table I, perfect signal reconstruction can be achieved, which we validate in both narrow-band and wide-band scenarios.

Effect of B. We fix the DR gain $\frac{\|f\|_\infty}{\lambda} = 10$ and number of channels $L = 72$ and increase $B = \frac{\Omega}{2\pi}$ from 2.45 Hz to 281.90 Hz. For each experiment, we compute the maximum frequency estimation error $\max_k |\omega_k - \widetilde{\omega}_k|$ by averaging 1000 independent realizations with random phase $\angle c_k$ (fixed $|c_k|$). Fig. 3 reveals how the frequency estimation error changes over different bandwidths. In all realizations, the estimation error falls below the error bound calculated in (4), which provides a quantitative predictor of the carrier frequency estimation error. This effectively validate Theorem 2.

IV. Conclusion

In this paper, we have proposed a novel method for blind multiband spectrum recovery from sub-Nyquist, modulo samples. By leveraging channel redundancy, our method enables perfect signal reconstruction in the absence of spectrum support information. Furthermore, we provide the theoretical bounds and hypotheses for spectrum support estimation in the presence of two kinds of non-linear folding in both amplitude and domain dimension. The proof of our theorem is constructive and leads to an efficient algorithm, which we validate in various conditions. With theoretical guarantees, our work opens up new capabilities for the field. Our algorithmic machinery directly enables sub-Nyquist applications such as cognitive radio [1], optical fiber communication [34] and RF communications [35] in the context of USF. Furthermore, our work facilitates towards new directions including, a) bandwidth-extension of modulo ADCs designed for lower sampling rates, b) robust algorithms benchmarking with hardware validation, c) investigation of new sampling architectures and recovery approaches that can further tighten the error bounds.

References

[1] D. Cohen and Y. C. Eldar, "Sub-Nyquist sampling for power spectrum sensing in cognitive radios: A unified approach," *IEEE Trans. Sig. Proc.*, vol. 62, no. 15, pp. 3897–3910, Aug. 2014.

[2] M. Mishali and Y. Eldar, "Blind multiband signal reconstruction: Compressed sensing for analog signals," *IEEE Trans. Sig. Proc.*, vol. 57, no. 3, pp. 993–1009, Mar. 2009.

[3] T. Darcie, "Subcarrier multiplexing for lightwave networks and video distribution systems," *IEEE J. Sel. Areas Commun.*, vol. 8, no. 7, pp. 1240–1248, 1990.

[4] J. Bingham, "Multicarrier modulation for data transmission: an idea whose time has come," *IEEE Commun. Mag.*, vol. 28, no. 5, pp. 5–14, May 1990.

[5] P. P. Vaidyanathan and P. Pal, "Sparse sensing with co-prime samplers and arrays," *IEEE Trans. Sig. Proc.*, vol. 59, no. 2, pp. 573–586, Feb. 2011.

[6] R. Venkataramani and Y. Bresler, "Optimal sub-Nyquist nonuniform sampling and reconstruction for multiband signals," *IEEE Trans. Sig. Proc.*, vol. 49, no. 10, pp. 2301–2313, Oct. 2001.

[7] ——, "Perfect reconstruction formulas and bounds on aliasing error in sub-Nyquist nonuniform sampling of multiband signals," *IEEE Trans. Inf. Theory*, vol. 46, no. 6, pp. 2173–2183, 2000.

[8] ——, "Further results on spectrum blind sampling of 2d signals," in *IEEE Intl. Conf. on Acoustics, Speech and Signal Processing (ICASSP)*, ser. ICIP-98, vol. 2. IEEE Comput. Soc, Oct. 1998, pp. 752–756.

[9] P. Feng and Y. Bresler, "Spectrum-blind minimum-rate sampling and reconstruction of multiband signals," in *IEEE Intl. Conf. on Acoustics, Speech and Signal Processing (ICASSP)*, ser. ICASSP-96, vol. 3. IEEE, May 1996, pp. 1688–1691.

[10] Y. Zhu, R. Guo, P. Zhang, and A. Bhandari, "Frequency estimation via sub-Nyquist unlimited sampling," in *Proc. IEEE Int. Conf. Acoust., Sig. Proc.* IEEE, Apr. 2024.

[11] V. Pavlíček, R. Guo, and A. Bhandari, "Bits, channels, frequencies and unlimited sensing: Pushing the limits of Sub-Nyquist Prony," in *European Sig. Proc. Conf. (EUSIPCO)*. IEEE, Aug. 2024, pp. 2462–2466.

[12] R. Guo, Y. Zhu, and A. Bhandari, "Sub-Nyquist USF spectral estimation: K frequencies with $6K + 4$ modulo samples," *IEEE Trans. Sig. Proc.*, vol. 72, pp. 5065–5076, 2024.

[13] R. Vaughan, N. Scott, and D. White, "The theory of bandpass sampling," *IEEE Trans. Sig. Proc.*, vol. 39, no. 9, pp. 1973–1984, 1991.

[14] Y.-P. Lin and P. Vaidyanathan, "Periodically nonuniform sampling of bandpass signals," *IEEE Trans. Circuits Syst. II*, vol. 45, no. 3, pp. 340–351, Mar. 1998.

[15] H. J. Landau, "Necessary density conditions for sampling and interpolation of certain entire functions," *Acta Math.*, vol. 117, no. 0, pp. 37–52, 1967.

[16] Y. Bresler and P. Feng, "Spectrum-blind minimum-rate sampling and reconstruction of 2-d multiband signals," in *IEEE Intl. Conf. on Image Processing (ICIP)*, ser. ICIP-96, vol. 1. IEEE, Sep. 1996, pp. 701–704.

[24] M. Beckmann, A. Bhandari, and F. Krahmer, "The modulo radon transform: Theory, algorithms, and applications," *SIAM J. Imaging Sci.*, vol. 15, no. 2, pp. 455–490, Apr. 2022.

[17] C. Herley and P. W. Wong, "Minimum rate sampling and reconstruction of signals with arbitrary frequency support," *IEEE Trans. Inf. Theory*, vol. 45, no. 5, pp. 1555–1564, Jul. 1999.

[18] A. Bhandari, F. Krahmer, and R. Raskar, "On unlimited sampling," in *International Conference on Sampling Theory and Applications (SampTA)*, Jul. 2017.

[19] ——, "On unlimited sampling and reconstruction," *IEEE Trans. Sig. Proc.*, vol. 69, pp. 3827–3839, Dec. 2020.

[20] A. Bhandari, F. Krahmer, and T. Poskitt, "Unlimited sampling from theory to practice: Fourier-Prony recovery and prototype ADC," *IEEE Trans. Sig. Proc.*, pp. 1131–1141, Sep. 2021.

[21] A. Bhandari, "Back in the US-SR: Unlimited sampling and sparse super-resolution with its hardware validation," *IEEE Signal Processing Letters*, vol. 29, pp. 1047–1051, Mar. 2022.

[22] R. Guo and A. Bhandari, "ITER-SIS: Robust unlimited sampling via iterative signal sieving," in *Proc. IEEE Int. Conf. Acoust., Speech, Sig. Proc.* IEEE, Jun. 2023.

[23] T. Feuillen, B. Shankar MRR, and A. Bhandari, "Unlimited sampling radar: Life below the quantization noise," in *Proc. IEEE Int. Conf. Acoust., Speech, Sig. Proc.* IEEE, Jun. 2023.

[25] Z. Liu, A. Bhandari, and B. Clerckx, "λ-MIMO: Massive MIMO via modulo sampling," *IEEE Trans. Commun.*, pp. 1–1, 2023.

[26] G. Shtendel, D. Florescu, and A. Bhandari, "Unlimited sampling of bandpass signals: Computational demodulation via undersampling," *IEEE Trans. Sig. Proc.*, vol. 71, pp. 4134–4145, 2023.

[27] S. Kay and S. Marple, "Spectrum analysis—a modern perspective," *Proc. IEEE*, vol. 69, no. 11, pp. 1380–1419, 1981.

[28] P. Stoica and A. Nehorai, "Music, maximum likelihood, and cramer-rao bound," *IEEE Trans. Acoust., Speech, Signal Process.*, vol. 37, no. 5, pp. 720–741, May 1989.

[29] T. Blu, P.-L. Dragotti, M. Vetterli, P. Marziliano, and L. Coulot, "Sparse sampling of signal innovations," *IEEE Signal Process. Mag.*, vol. 25, no. 2, pp. 31–40, 2008.

[30] Y.-X. Yao and S. Pandit, "Cramer-Rao lower bounds for a damped sinusoidal process," *IEEE Trans. Sig. Proc.*, vol. 43, no. 4, pp. 878–885, Apr. 1995.

[31] R. Guo and T. Blu, "FRI sensing: Retrieving the trajectory of a mobile sensor from its temporal samples," *IEEE Trans. Sig. Proc.*, vol. 68, pp. 5533–5545, 2020.

[32] Y. Li, R. Guo, T. Blu, and H. Zhao, "Generic FRI-based DOA estimation: A model-fitting method," *IEEE Trans. Sig. Proc.*, vol. 69, pp. 4102–4115, 2021.

[33] R. Guo, Y. Li, T. Blu, and H. Zhao, "Vector-FRI recovery of multi-sensor measurements," *IEEE Trans. Sig. Proc.*, vol. 70, pp. 4369–4380, 2022.

[34] T. Obtsuki, "Multiple-subcarrier modulation in optical wireless communications," *IEEE Commun. Mag.*, vol. 41, no. 3, pp. 74–79, Mar. 2003.

[35] J. Armstrong, "OFDM for optical communications," *J Lightwave Technol*, vol. 27, no. 3, pp. 189–204, Feb. 2009.